Electronic Supplementary Material (ESI) for New Journal of Chemistry.

A difluoroboron compound with latent fingerprint detection and inkless writing based on aggregation-induced emission enhancement and mechanofluorochromic behavior

Shufan Yang[1,a], Jiazhuang Tian[1,a], Bangcui Zhang[a], Yanhua Yang[a*], Xiangguang Li[a**], Shulin Gao[a***], Lin Shao[b], Fumin Li[c****]

[a] *School of Chemistry and Chemical Engineering, Kunming University, Kunming, 650214, P. R. China.*

[b] *Chromatographic Analysis Center, Dali Institute for Food Control, Dali, 671000, P. R. China.*

[c] *Physical and Chemical Inspection Center, Dali Institute for Food Control, Dali, 671000, P. R. China.*

Content

* Correspond author, E-mail address: yh_yangkmu@126.com (Y. Yang)
276090212@qq.com (X. Li)
778144294@qq.com (S. Gao)
810944654@qq.com (F. Li)

[1] The authors contribute equally to this paper.

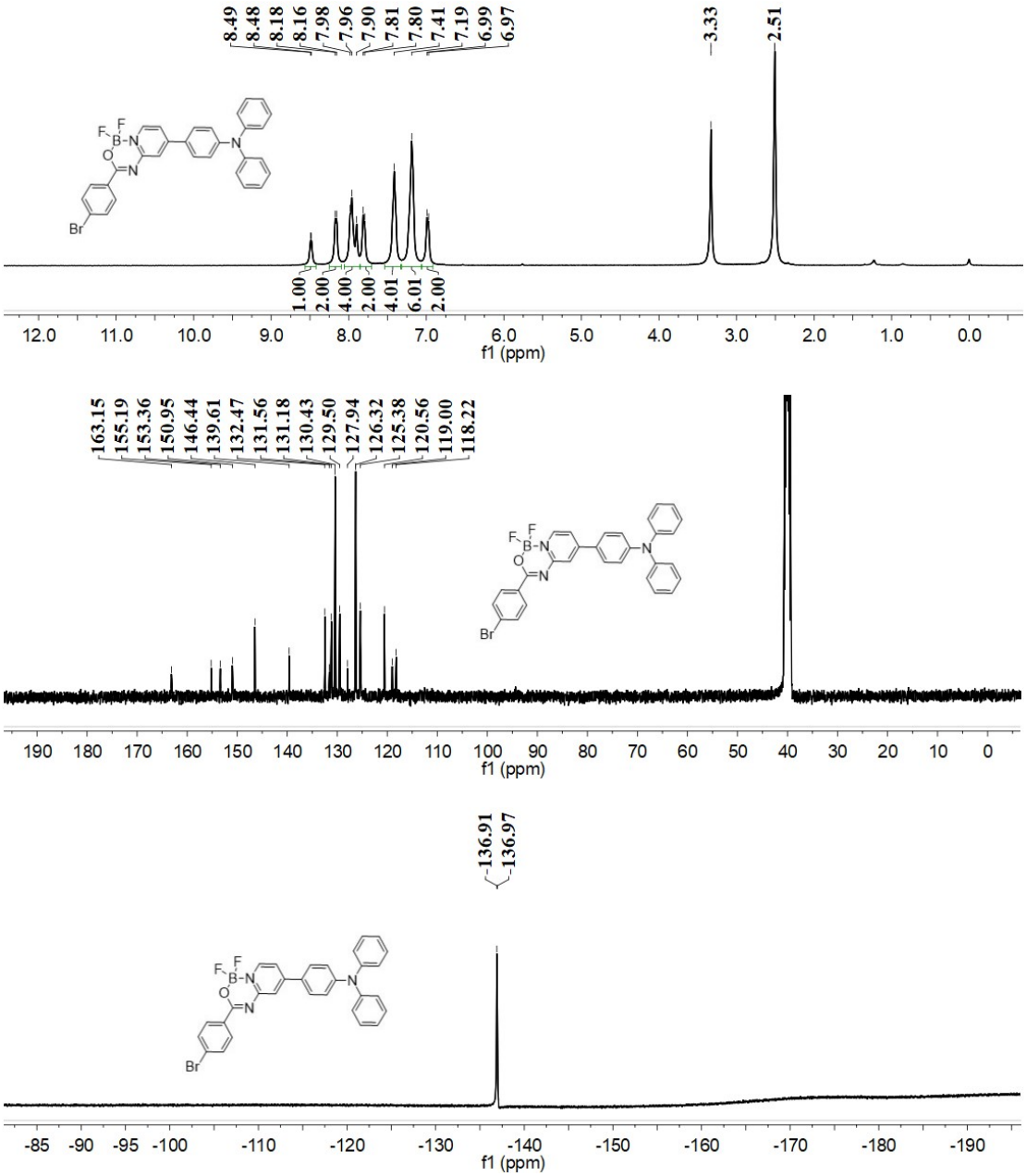

Figure S1 ^{1}H NMR, ^{13}C NMR and ^{19}F NMR spectra of **TPA-Py-Br BF_2** in DMSO-d_6.

User Spectra

Fragmentor Voltage	Collision Energy	Ionization Mode
135	0	ESI

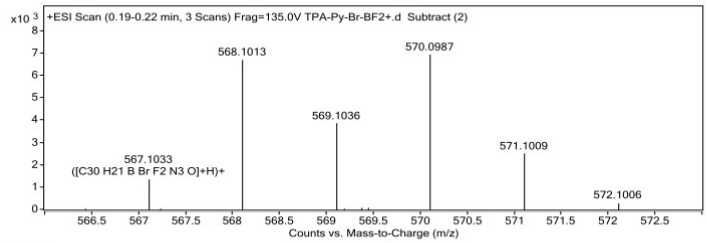

Peak List

m/z	z	Abund
568.1013	1	6742.59
569.1036	1	3881.47
570.0987	1	6971.85
571.1009	1	2529.42
1137.1905	1	2929.7
1138.1929	1	2062.52
1139.1909	1	1867.06
1159.1737	1	2344.03
1175.1489	1	1860.57
1176.1481	1	1679.35

Formula Calculator Element Limits

Element	Min	Max
C	3	60
H	0	50
O	0	5
Br	0	2
N	0	5
F	0	3
B	1	1

Formula Calculator Results

Formula	CalculatedMass	CalculatedMz	Mz	Diff. (mDa)	Diff. (ppm)	DBE
C30 H21 B Br F2 N3 O	566.0965	567.1038	567.1033	0.5	0.8	21.0000

Figure S2 HRMS of **TPA-Py-Br BF_2**.

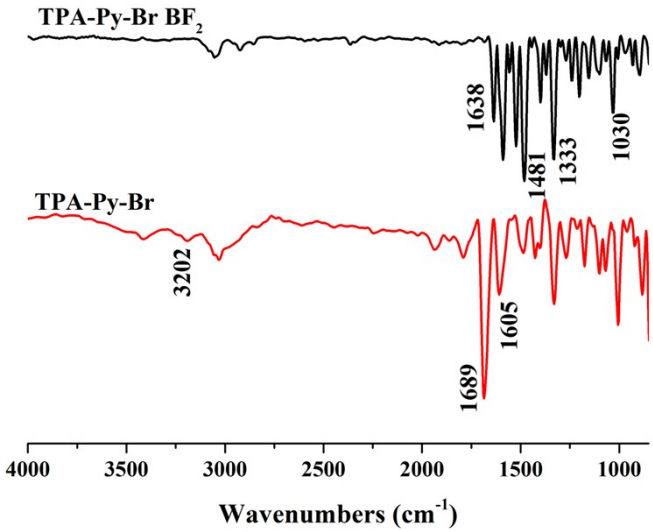

Figure S3 FTIR of **TPA-Py-Br** and **TPA-Py-Br BF_2**.

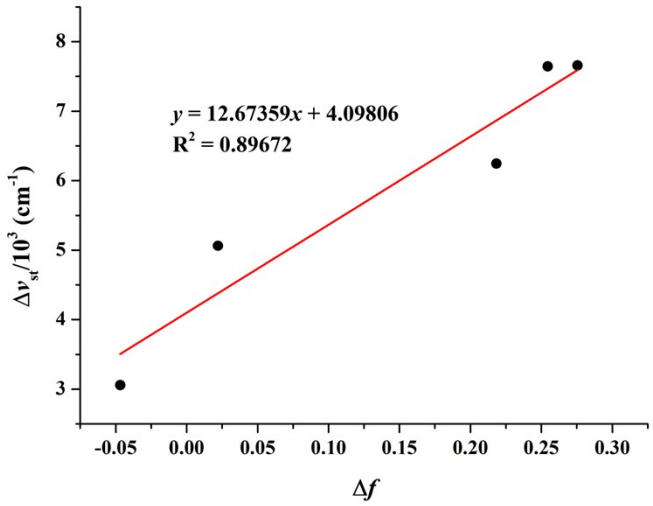

Figure S4 Lippert-Mataga plot of **TPA-Py-Br BF_2** in different solvents.

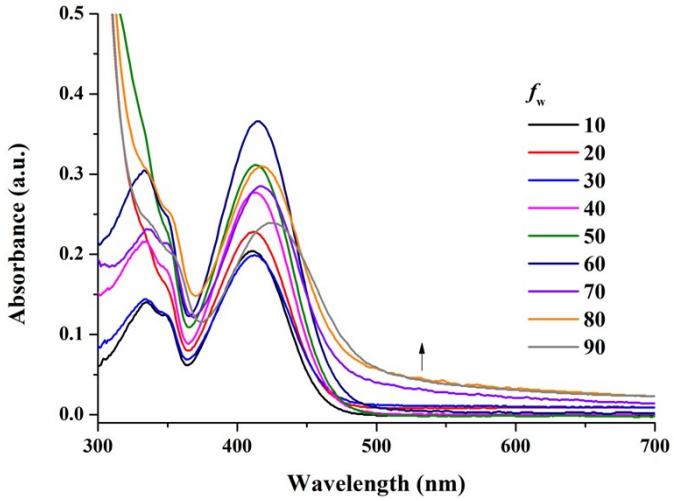

Figure S5 Absorption spectra of **TPA-Py-Br BF_2** in THF and H_2O mixtures (c = 1.0 × 10^{-5} mol/L)

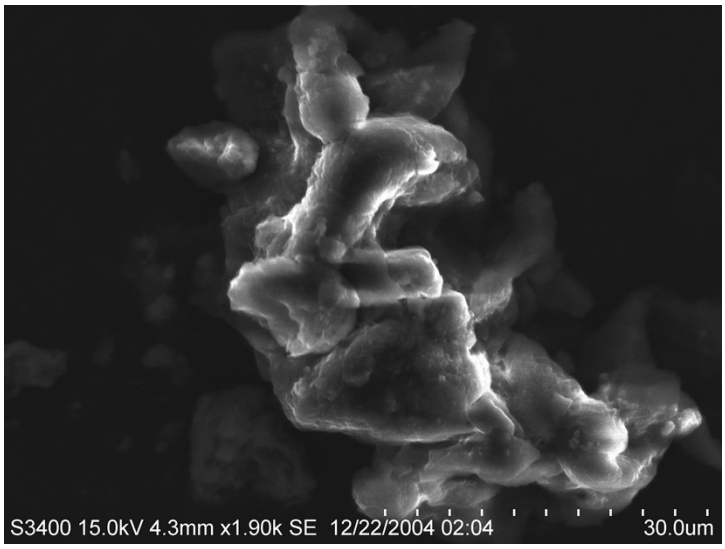

Figure S6 SEM images of **TPA-Py-Br BF_2** in THF/H_2O mixture (f_w = 80%)

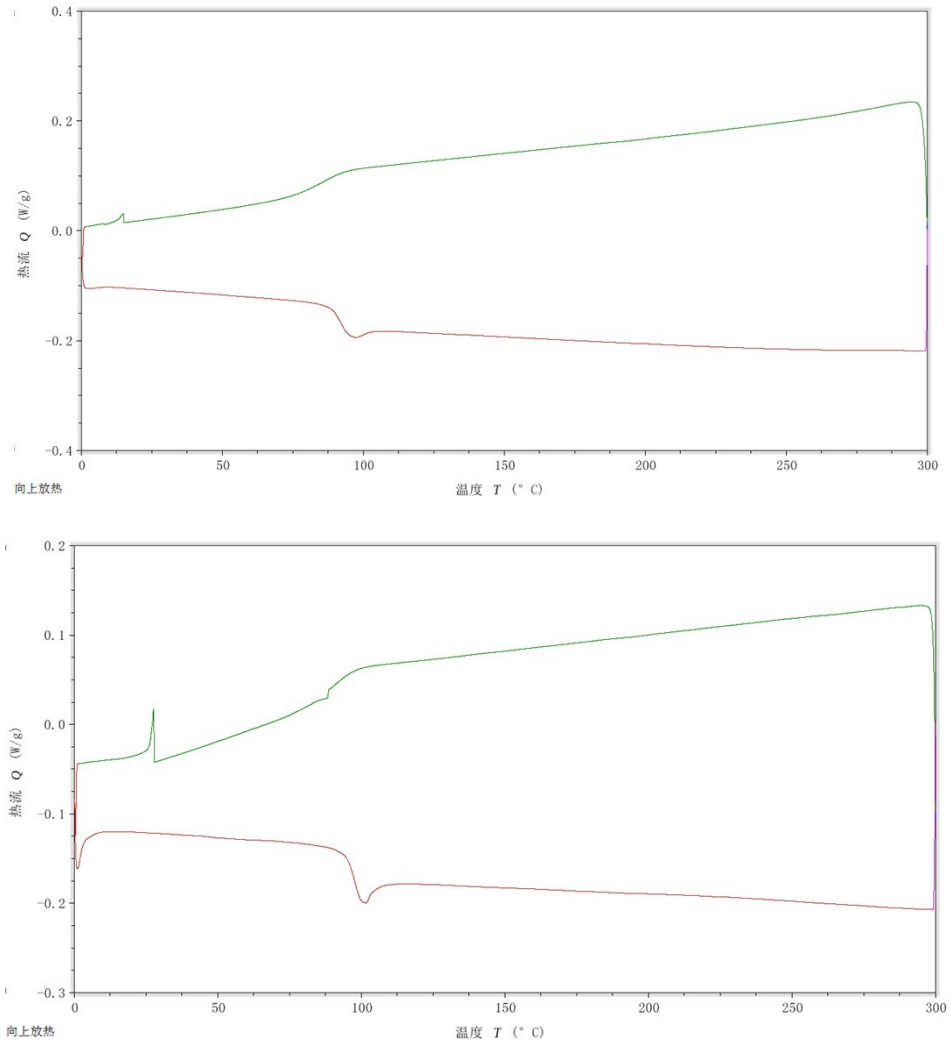

Figure S7 DSC curves of **TPA-Py-Br BF_2** before (up) and after grinding (down), respectively.

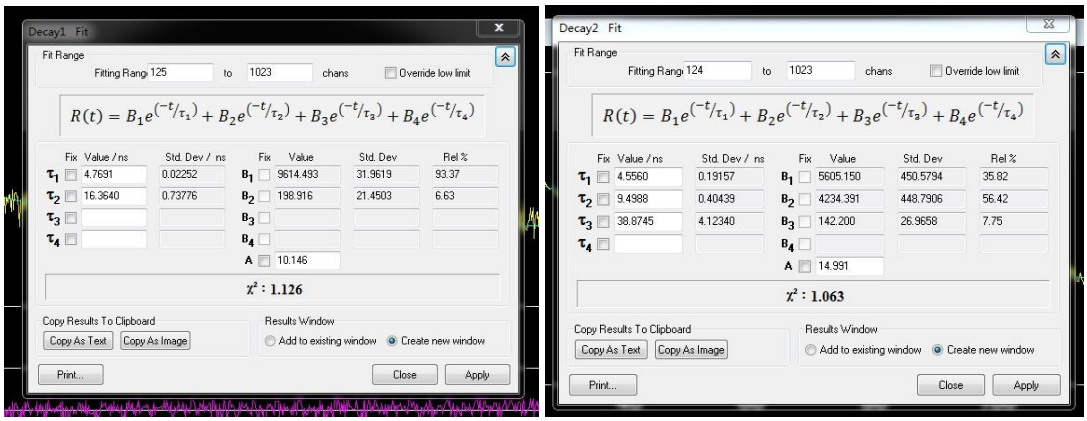

Figure S8 τ of **TPA-Py-Br BF_2** before (up) and after grinding (down), respectively.

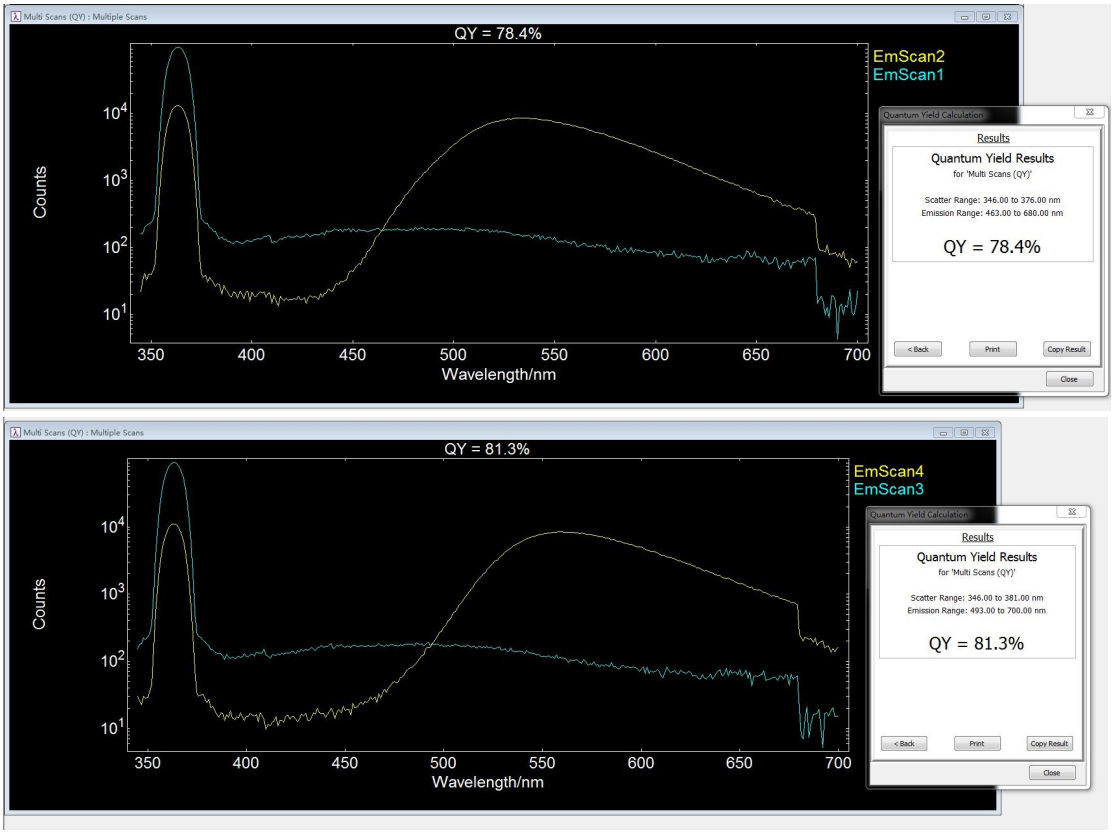

Figure S9 Φ_f of **TPA-Py-Br BF_2** before (up) and after grinding (down), respectively.

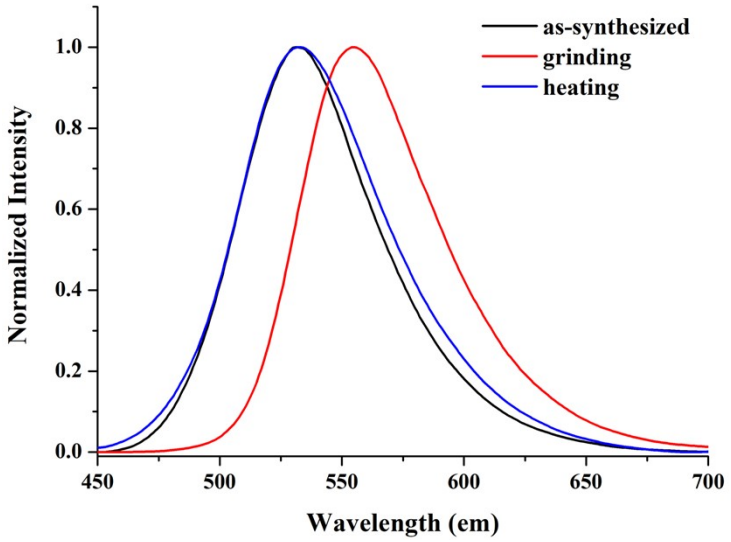

Figure S10 Normalized emission spectra (λ_{ex} = 365 nm) of **TPA-Py-Br BF_2** before and after grinding, and after heating, respectively.

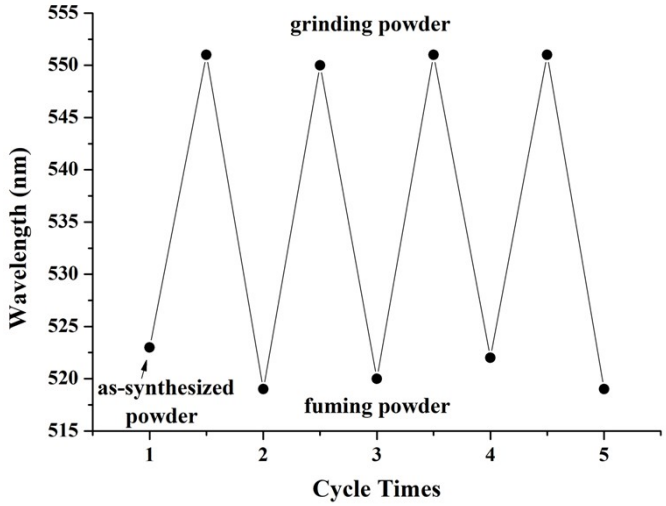

Figure S11 The emission wavelength of **TPA-Py-Br BF_2** upon treated by grinding and fuming with CH_2Cl_2 repeatedly.

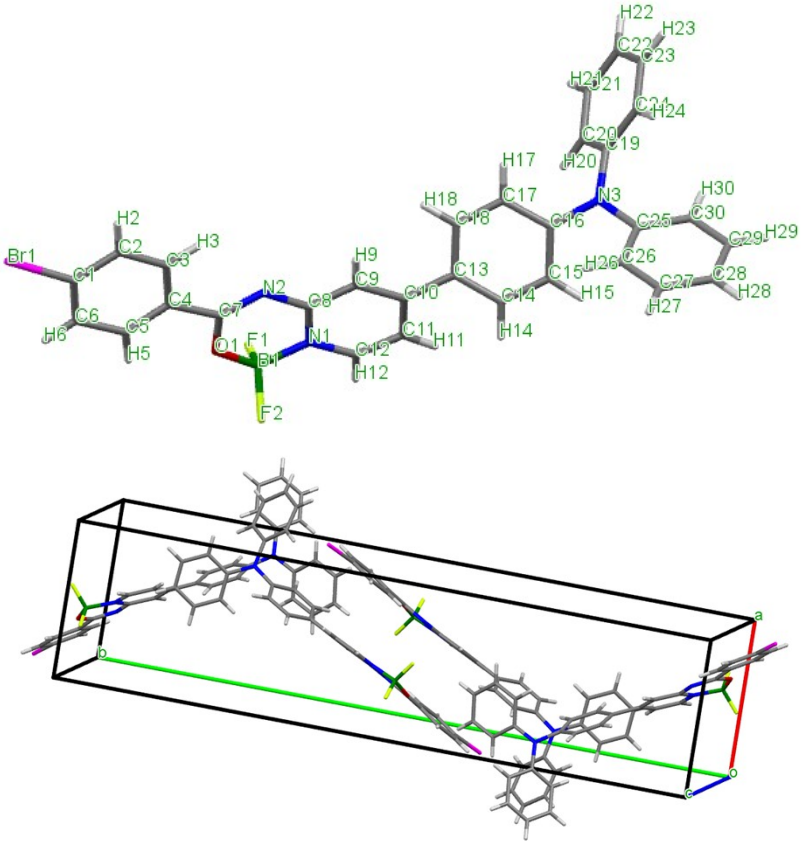

Figure S12 The molecular conformation of **TPA-Py-Br BF_2** in front view and unit cell in single crystal.

Table S1 Photophysical data of compound **TPA-Py-Br BF_2** in various organic solvents

Compound	Solvents	Δf [a]	λ_{abs}/nm	λ_{em}/nm	$\Delta\nu_{st}$ [b]/10^3 cm^{-1}
TPA-Py-Br BF_2	*n*-hexane	-0.0468	274, 331, 345, 401	457	3.057
	PhCl	0.0222	337, 416	527	5.063
	CH_2Cl_2	0.2185	272, 335, 415	562	6.044
	DMF	0.2756	334, 413	604	7.657
	DMSO	0.2545	273, 336, 416	610	7.645

[a] Δf refered to solvent polarity parameters, it was calculated as follows:

$$\Delta f = \frac{\varepsilon - 1}{2\varepsilon + 1} - \frac{n^2 - 1}{2n^2 + 1}$$

where ε was the static dielectric constant, *n* was the optical refractive index of the solvent.

[b] $\Delta\nu_{st} = \Delta\nu_{abs} - \Delta\nu_{em}$

Table S2. Crystal data and structure refinement for **TPA-Py-Br BF_2**.

Identification code	cu_20230614_YS_KMXY_SF_4_0m
Empirical formula	$C_{30}H_{21}BBrF_2N_3O$
Formula weight	568.22
Temperature/K	193.00
Crystal system	monoclinic
Space group	$P2_1/c$
a/Å	8.2149(4)
b/Å	33.6377(13)
c/Å	9.9837(4)
α/°	90
β/°	90.872(3)
γ/°	90
Volume/Å^3	2758.5(2)
Z	4

$\rho_{calc}g/cm^3$	1.368
μ/mm^{-1}	2.374
F(000)	1152.0
Crystal size/mm^3	0.13 × 0.11 × 0.1
Radiation	CuKα (λ = 1.54178)
2Θ range for data collection/°	9.24 to 136.414
Index ranges	-9 ≤ h ≤ 9, -39 ≤ k ≤ 39, -12 ≤ l ≤ 12
Reflections collected	26871
Independent reflections	4979 [R_{int} = 0.0775, R_{sigma} = 0.0623]
Data/restraints/parameters	4979/75/438
Goodness-of-fit on F^2	1.090
Final R indexes [I>=2σ (I)]	R_1 = 0.0791, wR_2 = 0.1822
Final R indexes [all data]	R_1 = 0.1121, wR_2 = 0.2004
Largest diff. peak/hole / e $Å^{-3}$	0.42/-0.34

Theoretical calculations

Quantum chemical calculation results were studied from the density functional theory (DFT) using B3LYP/6-31G(d) and TD-CAM-B3LYP/6-31G(d) level for the ground and excited states[1], respectively, through the Gaussian 09 program package[2], and the frontier molecular orbital and electrostatic potential (ESP) surface were obtained by Multiwfn 3.8(dev)[3,4] and visual molecular dynamic (VMD) software[5], respectively.

References

[1] Yanai T, Tew D P, Handy N C. A new hybrid exchange–correlation functional using the Coulomb-attenuating method (CAM-B3LYP) [J]. Chemical physics letters, 2004, 393(1-3): 51-57.

[2] Frisch M J, Trucks G W, Schlegel H B, Scuseria G E, Robb M A, Cheeseman J R, Scalmani G, Barone V, Petersson G A, Nakatsuji H, Li X, Caricato M, Marenich A V, Bloino J, Janesko B G, Gomperts R, Mennucci B, Hratchian H P, Ortiz J V, Izmaylov A F, Sonnenberg J L, Williams, Ding F, Lipparini F, Egidi F, Goings J, Peng B, Petrone A, Henderson T, Ranasinghe D, Zakrzewski V G, Gao J, Rega N, Zheng G, Liang W, Hada M, Ehara M, Toyota K, Fukuda R, Hasegawa J, Ishida M, Nakajima T, Honda Y, Kitao O, Nakai H, Vreven T, Throssell K, Montgomery Jr. J A, Peralta J E, Ogliaro F, Bearpark M J, Heyd J J, Brothers E N, Kudin K N, Staroverov V N, Keith T A, Kobayashi R, Normand J, Raghavachari K, Rendell A

P, Burant J C, Iyengar S S, Tomasi J, Cossi M, Millam J M, Klene M, Adamo C, Cammi R, Ochterski J W, Martin R L, Morokuma K, Farkas O, Foresman J B, Fox D J. Gaussian 16 Rev. A.03 [M]. Wallingford, CT; Gaussian, Inc. 2016.

[3] Zhang J, Lu T. Efficient evaluation of electrostatic potential with computerized optimized code [J]. Physical Chemistry Chemical Physics, 2021, 23(36): 20323-20328.

[4] Lu T, Chen F. Multiwfn: a multifunctional wavefunction analyzer [J]. Journal of computational chemistry, 2012, 33(5): 580-592.

[5] Humphrey W, Dalke A, Schulten K. VMD: visual molecular dynamics [J]. Journal of molecular graphics, 1996, 14(1): 33-38.